

## Minimal model for avalanches in granular systems

Stefan J. Linz and Peter Hänggi

*Theoretische Physik I, Institut für Physik, Universität Augsburg, D-86135 Augsburg, Germany*

(Received 24 February 1994)

A nonlinear model for the dynamics of avalanches in granular systems is presented. It is based on mean-field equations for the particle velocity and the angle of the surface of the granular system. The friction force is discontinuous at zero velocity and increases monotonically with the square of the velocity. The model explains the main features of the dynamics of avalanches in analytical detail. It also explains the logarithmic decay behavior of the angle of the pile in the presence of vibrations as found experimentally by Jaeger *et al.* [Phys. Rev. Lett. **62**, 40 (1990)].

PACS number(s): 46.10.+z, 81.35.+k

### INTRODUCTION

Granular systems (e.g., sand or dry coffee powder) are large assemblies of grains which interact only by repulsive forces due to collisions and friction. Recent experiments have shown that this state of matter shows many surprising and not yet understood features [1–5] such as dilatancy, bistability, size segregation, convective transport, and pattern formation. In particular, granular systems exhibit solid-like properties when they deform plastically under weak shear, but also fluidlike properties since they can flow in a non-Newtonian manner under high shear [1]. The understanding of this behavior is not only of fundamental interest in physics; it also has widespread applications for chemical engineering and geophysics [1].

The reason why granular systems can start to flow and stop again is an elementary and *fundamental* problem. Recently, several experimental [2–6], numerical [7], as well as theoretical approaches [6,8,9] have been reported. The typical experimental setup is a pile of grains (e.g., glass spheres) in a horizontal cylinder or drum, which can also be rotated about its axis with a constant angular velocity. The slope of the pile is characterized by the angle  $\varphi$  measured with respect to the horizontal. Some important experimental findings [2,6] are the following. (i) Without rotation, there is a maximum angle of repose  $\varphi_s$  below which the pile is at rest. For larger angles, an avalanche flows until the pile comes to rest again at a minimum angle of repose  $\varphi_r < \varphi_s$ . (ii) With external rotation, two types of dynamics are possible: periodic slip-stick behavior (alteration between avalanches and rest states) for small rotation rates and constant flow above a threshold rotation rate  $\omega_T$ . (iii) A logarithmic decay behavior of the angle in time occurs if the pile is driven by external vertical vibrations. In all these experiments the dynamics of the pile is mainly concentrated in a thin layer of grains at the surface. The model that we present, explains *in analytical detail all three features in a unified way on the basis of a nonlinear oscillator model*. It shows that many properties of avalanches can be understood in a “deterministic” way without knowing the “mesoscopic” details of the system.

### BASICS

Phenomenologically, one can describe the dynamics of avalanches by a system of coupled dynamical equations [6,8,9] for the velocity of a grain at the surface of the avalanche in the mean field of the others  $v(t)$  and slope of the surface of the pile  $\varphi(t)$ . Here  $v$  and  $\varphi$  are quantities averaged over an ensemble of experiments. The static behavior of the pile can be modeled as follows: If  $v \equiv 0$  and  $\varphi \leq \varphi_s$ , the rest state is stable [6]. The dynamic behavior can be described in analogy to Coulomb's theory of friction of a body on an inclined plane. The force balance requires that the acceleration of a grain is determined by the sum of the tangential component of the gravity force, proportional to  $\sin\varphi$ , and the friction force, proportional to  $k_d(v)\cos\varphi$  as proposed by Jaeger *et al.* [8]. In this one-dimensional picture, the dynamical friction coefficient  $k_d(v)$  accounts for all the friction and collision effects that the grain undergoes, and depends on the velocity.

For large  $v$ , it is well known [1,6,8] that Bagnold's law [10] holds, i.e.,  $k_d(v)$  increases proportional to  $v^2$ . In the previous literature, two proposals have been put forth for the velocity dependence of  $k_d(v)$  for small  $v$ : (i) Jaeger *et al.* [8] suggest that  $k_d(v) = a_1/(1 - a_2v^2) + a_3v^2$  with  $a_1 > 0, a_3 > 0$ , and  $a_1a_2 + a_3 < 0$ ; (ii) Caponeri *et al.* [6] use  $k_d(v) = c_0 - c_1v + c_2v^2$  with  $v \geq 0$  and  $c_i > 0$  ( $i=0,1,2$ ). In both cases, the authors assume that  $k_d(v)$  exhibits a minimum for small, nonzero velocities (implying a region of negative differential friction) and increases for larger velocities according to Bagnold's law. In contrast, we suppose a monotonically increasing dynamical friction coefficient  $k_d(v)$  is, with  $b_0 > 0$  and  $b_2 > 0$ , of the form

$$k_d(v) = b_0 + b_2v^2 \quad \text{if } v > 0. \quad (1)$$

The static limit of the dynamic friction coefficient  $k_d(v \rightarrow 0)$  corresponds to an angle  $\varphi_d = \arctan(b_0)$  [11]. This angle is smaller than the maximum angle of repose  $\varphi_s$ , so that there is a discontinuity at zero velocities [6]. In the following, we will demonstrate that (i) the choice of a dynamic friction coefficient  $k_d(v)$ , which *increases*

monotonically with  $v^2$ , and (ii) the discontinuous behavior when switching from static to dynamic, are *sufficient* to explain the characteristic stick-slip and constant flow behavior of avalanches [2,6]. It can also explain the  $\ln(t)$  relaxation of  $\varphi$  in the presence of vibrations [2].

In an avalanche, the dynamics of  $\varphi$  is coupled to the velocity by  $\dot{\varphi}=f(\varphi,v)$ . Without flow ( $v=0$ ), no changes of the angle are possible. Thus one obtains, in the lowest-order approximation,  $\dot{\varphi}=-av$ , with a coupling parameter  $a>0$  as proposed by Caponeri *et al.* [6] and Benza, Nori, and Pla [9]. Of course,  $a$  can also depend on  $\varphi$  [9]. This, however, is not a leading-order effect in the following discussion, except for the influence of vibrations discussed at the end of this paper.

### MODEL EQUATIONS

For the sake of simplicity, we restrict the discussion to positive angles  $\varphi$ . The combination of the static and dynamic force balance and the friction law (1), as well as incorporation of additional external rotation, leads to

$$\dot{v}=g[\sin\varphi-(b_0+b_2v^2)\cos\varphi]\chi(\varphi,v), \quad (2a)$$

$$\dot{\varphi}=-av+\bar{\omega}, \quad (2b)$$

with the cutoff function being  $\chi(\varphi,v)=\Theta(v)+\Theta(\varphi-\varphi_s)-\Theta(v)\Theta(\varphi-\varphi_s)$ . Here  $\Theta$  denotes the step function [ $\Theta(y)=0$  (1) if  $y\leq 0$  ( $y>0$ )]. The cutoff function  $\chi$  guarantees that the system stays at rest as long as  $v=0$  and  $\varphi\leq\varphi_s$  and it is trapped at the state of rest, when  $v$  goes to zero and  $\varphi\leq\varphi_s$ .  $\bar{\omega}$  denotes the positive-valued constant external rotation rate. Equations (2a) and (2b) apply only to *grains at the surface of the pile*. Grains in the bulk underlie additional constraints due to the grains on top of them. Therefore, the thickness of the surface boundary layer of grains moving with the avalanche cannot be described within our approach. For a satisfactory description of the boundary layer effects one has to consider field theoretical approaches, which are beyond the scope of our present objective.

All dynamics of avalanches are basically centered around the angle  $\varphi_d$ . Introducing the deviation from this angle, i.e.,  $\Phi(t)=\varphi(t)-\varphi_d$ , scaling time as  $t\rightarrow t/\sqrt{ga}$  and the velocity as  $v\rightarrow v\sqrt{g/a}$  and setting  $\omega=\bar{\omega}/\sqrt{ga}$ , one can transform (2) to an equivalent second-order equation in  $\Phi$ :

$$\ddot{\Phi}-[\delta(\cos\Phi-\mu\sin\Phi)(\dot{\Phi}-\omega)^2-\Omega_0^2\sin\Phi]\chi(\Phi,\dot{\Phi})=0, \quad (3)$$

where  $\chi(\Phi,\dot{\Phi})=\Theta(-\dot{\Phi}+\omega)+\Theta(\Phi-\Phi_s)-\Theta(-\dot{\Phi}+\omega)\Theta(\Phi-\Phi_s)$ ,  $\Phi_s=\varphi_s-\varphi_d$ ,  $\delta=(gb_2/a)\cos\varphi_d>0$ ,  $\mu=\tan\varphi_d$ , and  $\Omega_0^2=(1+\tan^2\varphi_d)\cos\varphi_d>0$ . Given the dynamics of  $\Phi$ , the velocity reads  $v=\omega-\dot{\Phi}$ . Note that  $\Omega_0^2$  depends only on  $\varphi_d$  and is of order unity for not too large angles  $\varphi_d$ . The parameter  $\delta$ , however, is proportional to the ratio  $b_2/a$  of the curvature of the friction coefficient and the relaxation rate of the angle.

### NUMERICAL RESULTS

To demonstrate that our model shows the basic features of avalanches, we integrate (3) numerically. Fig-

ure 1 shows trajectories in the  $(\omega-\dot{\Phi},\Phi)$  phase space for three different values of  $\omega$ . Relevant initial conditions are  $v(0)=0$  and  $\Phi(0)$  infinitesimally above the maximum angle of repose  $\Phi_s$ . For  $\omega=0$  [Fig. 1(a)], the angle  $\Phi(t)$  decreases monotonically. The velocity  $v(t)$  increases first, since the velocity-dependent part of the friction is still small. Then the Bagnold friction becomes dominant and slows down the motion until the minimum angle of repose  $\Phi_r$ , with  $v=0$ , is reached. For  $\omega\neq 0$ , e.g.,  $\omega=0.05$  [Fig. 1(b)], the behavior is different. Due to external rotation,  $\Phi(t)$  and  $v(t)$  increase first, until the Bagnold friction slows down the motion to end up at  $v=0$  and  $\Phi_r$ . Before reaching  $v=0$ , the angle  $\Phi$  increases again. The

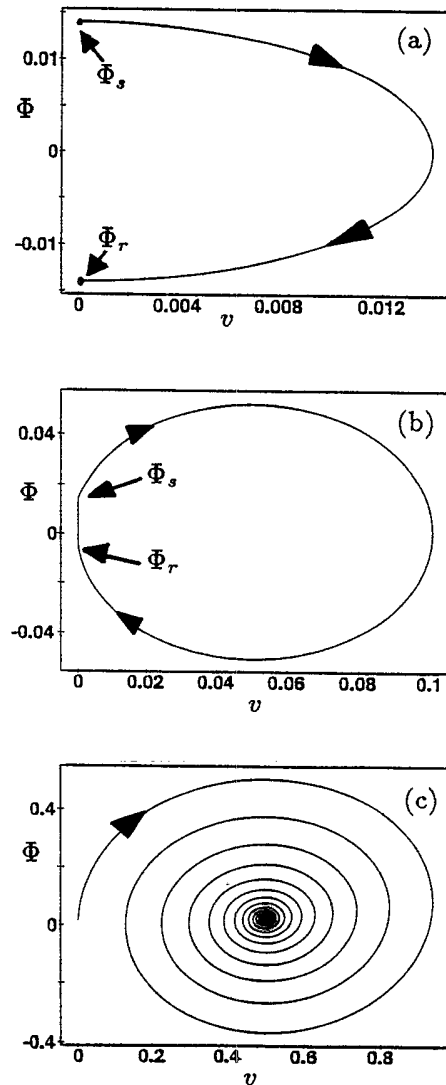


FIG. 1. Trajectories of Eq. (3) in the phase-space spanned by  $v$  and  $\Phi$  for three different external rotation rates (a)  $\omega=0$ , (b)  $\omega=0.05$ , and (c)  $\omega=0.5$ . The parameters  $\varphi_s$  and  $b_0$  that we have chosen are extrapolations of the experiment of Ref. [2]:  $\varphi_s=0.48$  (corresponding to a maximum angle of repose of  $27.8^\circ$ ) and  $b_0=0.503$  (corresponding to  $\varphi_d=26.7^\circ$ ). This implies that  $\Omega_0^2\approx 1$ . Since  $a$  and  $b_2$  are not known, we have chosen a representative value  $\delta=0.1$ .

system is still insensitive enough to end up in the rest state. It stays at rest until it reaches  $\Phi_s$  again. Then the next avalanche starts. Above a threshold value  $\omega_T=0.053$ ... (given by the condition that the trajectory ends in  $\Phi_r=0$ ), the dynamics changes topologically. For  $\omega=0.5$  [Fig. 1(c)], the system approaches the fixed point  $\Phi_{st}=\arctan[\delta\omega^2/(\Omega_0^2-\mu\delta\omega^2)]$  in form of a spiral. The dynamical behavior of (3) agrees well with the experiments in Refs. [2,6]. Qualitatively similar behavior has also been observed numerically in the model [6] with non-monotonic friction laws.

### A MINIMAL MODEL

To gain more insight into the physics of avalanches and to extract in analytical form the features of (3), we simplify the model as follows. With  $|\Phi(t)|$  being small, as it is in the relevant situation in the experiments [2,6], we can approximate  $\sin\Phi$  by  $\Phi$  and the term in front of  $(\dot{\Phi}-\omega)^2$  by unity to obtain the approximation

$$\ddot{\Phi}-[\delta(\dot{\Phi}-\omega)^2-\Omega_0^2\Phi]\chi(\Phi,\dot{\Phi})=0. \quad (4)$$

If  $\delta=0$  and  $v>0$  [i.e.,  $\chi(\Phi,\dot{\Phi})=1$ ], (4) reduces to an undamped harmonic oscillator. For nonzero  $\delta$  and  $v>0$ , it is a harmonic oscillator with nonlinear friction coefficient  $-\delta(2\omega-\dot{\Phi})$  and a constant external driving  $\delta\omega^2$ . Equation (4) constitutes our minimal model for the dynamics of avalanches. It is the lowest-order, nontrivial reduction of (3); for not too large  $\omega$ , it leads to predictions that agree within line thickness with the dynamics of (3). Throughout the following, we discuss analytically its main features.

### NO ROTATION

If  $\omega=0$  and  $v>0$ , the model (4) reduces with  $\Omega^2>0$  and  $\delta>0$  to a harmonic oscillator with a negative quadratic friction, i.e.,

$$\ddot{\Phi}-\delta\dot{\Phi}^2+\Omega_0^2\Phi=0 \quad \text{where } \dot{\Phi}<0. \quad (5)$$

The relevant initial conditions are  $\Phi(0)=\Phi_s$  and  $\dot{\Phi}(0)=0$ . For the moment, we discuss (5) without the constraint  $\dot{\Phi}<0$ . Its only fixed point  $\Phi=\dot{\Phi}=\ddot{\Phi}=0$  is elliptic. Therefore, the system in (5) possesses a periodic solution with a constant of motion reading explicitly

$$J=[\frac{1}{2}\dot{\Phi}^2-(\Omega_0^2/4\delta^2)(1+2\delta\Phi)]\exp(-2\delta\Phi). \quad (6)$$

For small  $\delta$ , the periodic solution can be obtained asymptotically by the use of a Poincaré-Lindstedt expansion [12]. The result is

$$\Phi(t)=\Phi_s\cos(\Omega t)+\delta\Phi_8(t)+O(\delta^2), \quad (7a)$$

$$\Phi_8(t)=\frac{1}{2}\Phi_s^2[1-\frac{4}{3}\cos(\Omega t)+\frac{1}{3}\cos(2\Omega t)], \quad (7b)$$

$$\Omega=\Omega_0[1-\delta^2\Phi_s^2/6+O(\delta^4)]. \quad (7c)$$

Note that the period  $T=2\pi/\Omega=(2\pi/\Omega_0)[1+\delta^2\Phi_s^2/6+O(\delta^4)]$  increases quadratically with increasing  $\delta$ .

For avalanches in granular media one also has to take into account the constraint  $\dot{\Phi}<0$  in (5), or equivalently

the cutoff function  $\chi$ . This implies the following. (i) Only the first half oscillation of the periodic solution is important. Once started at an angle  $\Phi_s$ , the avalanche slips until the velocity reaches  $v=-\dot{\Phi}=0$  at an angle  $\Phi_r$  and sticks there forever. (ii) The duration time of an avalanche is  $T_a=T/2$ . (iii) The maximum angle of repose  $\Phi_s$  determines the minimum angle of repose  $\Phi_r=-\Phi_s(1-\frac{4}{3}\delta\Phi_s)+O(\delta^2)$ . (iv) Minimum and maximum angles are  $\Phi_r$  and  $\Phi_s$ ; while slipping, no angle outside this range can be reached. (v) The maximum velocity of the avalanche  $v_{\max}$  is determined by the condition  $\dot{\Phi}^2=(\Omega_0^2/\delta)\Phi$ . Using the small- $\delta$  result, one obtains  $v_{\max}=\Phi_s\Omega_0[1-\frac{2}{3}\Phi_s\delta+O(\delta^2)]$  at time  $t(v_{\max})=(\pi/2\Omega_0)[1-(4/3\pi)\Phi_s\delta+O(\delta^2)]$  and at an angle  $\Phi(v_{\max})=\Phi_s^2\delta+O(\delta^2)$ . It occurs at an angle slightly above  $\varphi_d=(\varphi_s-\varphi_r)/2+O(\delta)$ . (vi) Since  $v_{\max}$  and  $\Phi(v_{\max})$  are experimentally measurable, one can fit the experimental data by the parameters  $\delta$  and  $\Omega_0^2$  of the model. They are related by  $\delta=\Phi(v_{\max})/\Phi_s^2$  and  $\Omega_0=(v_{\max}/\Phi_s)[1+(2/3)\Phi_s\delta+O(\delta^2)]$ .

### FINITE ROTATION RATE

The minimal model with  $\omega\neq 0$  and  $\chi(\Phi,\dot{\Phi})=1$  reads

$$\ddot{\Phi}-\delta(\dot{\Phi}-\omega)^2+\Omega_0^2\Phi=0 \quad \text{with } \dot{\Phi}-\omega<0. \quad (8)$$

Dropping momentarily the constraint  $\dot{\Phi}-\omega<0$  in (8), the dynamics is invariant under simultaneous reversal of time  $t\rightarrow -t$  and rotation rate  $\omega\rightarrow -\omega$ . Its only fixed point is given by  $\Phi_{st}=\delta(\omega/\Omega_0)^2$ . A linear stability analysis of the fixed point leads to eigenvalues  $\lambda_{1,2}=-\delta\omega[1\pm\sqrt{1-1/\Phi_{st}}]$ . Therefore,  $\Phi_{st}$  is linearly stable for all  $\delta>0$ . Its topology is a stable focus if  $\Phi_{st}<1$  and a stable node if  $\Phi_{st}>1$ . We conclude first that the periodic solution for  $\omega=0$  develops into a transient oscillatory approach to the fixed point  $\Phi_{st}$ , provided  $\Phi_{st}<1$ . Second, the model is dissipative for nonzero  $\delta$ , i.e., it no longer possesses a constant of motion. To obtain information on the transient approach of the fixed point for small  $\delta$ , we apply the method of averaging [12]. With the relevant initial conditions  $\Phi(0)=\Phi_s$  and  $\dot{\Phi}(0)=\omega$ , one obtains

$$\begin{aligned} \Phi(t) &= \Phi_{st} + (\Phi_s - \Phi_{st})\cos^{-1}(\alpha) \\ & \times \exp(-\delta\omega t)\cos(\Omega_0 t + \alpha), \end{aligned} \quad (9a)$$

$$\alpha = -\arctan \left[ \frac{\omega(\Omega_0^2 + \Phi_s\Omega_0^2\delta - \omega^2\delta^2)}{\Omega_0(\Phi_s\Omega_0^2 - \omega^2\delta)} \right]. \quad (9b)$$

Now taking into account the constraint  $\dot{\Phi}-\omega<0$ , the implications for avalanches in granular systems are the following. (i) For given  $\Omega_0$  and  $\delta>0$  and initial angle  $\Phi_s$ , there are a time  $t_T$  and a rotation rate  $\omega_T$  such that simultaneously  $\dot{\Phi}(t_T)=0=\Phi(t_T)$  and  $\dot{\Phi}(t_T)=\omega_T$  are fulfilled. At that rotation rate  $\omega_T$ , the transition between stick-slip and constant-flow behavior happens. Using (9), one can show that  $\omega_T$  is approximately given by the solution of the transcendental equation

$$\begin{aligned} & \frac{\omega_T}{\Omega_0} \cos \left[ \arctan \frac{\omega_T}{\Omega_0 \Phi_s} + \frac{\omega_T}{\Omega_0} \delta \right] \\ &= \left[ \Phi_s - \delta \frac{\omega_T^2}{\Omega_0^2} \right] \\ & \times \exp \left\{ -\delta \frac{\omega_T}{\Omega_0} \left[ \frac{3}{2} \pi + \arctan \frac{\omega_T}{\Omega_0 \Phi_s} \right] \right\}. \end{aligned}$$

For the numerical values discussed above (cf. Fig. 1), we obtain  $\omega_T \approx 0.054$ , which compares very well with the threshold value  $\omega_T = 0.053$  . . of (3). (ii) For  $\omega > \omega_T$ ,  $v(t) = \omega - \dot{\Phi}(t)$  is strictly positive for all times and the avalanche approaches the constant flow solution  $\Phi_{st}$  oscillatorily according to (9). The product  $\delta\omega$  corresponds to an inverse relaxation time and measures how quickly the avalanche reaches the constant flow solution  $\Phi_{st}$ . (iii) For  $\omega < \omega_T$ , the solution (9) will reach  $v=0$  after a finite time  $t_r$ , given by the condition  $v(t_r) = \omega - \dot{\Phi}(t_r) = 0$ , at a minimum angle of repose  $\Phi_r = \Phi(t_r)$ . From (9) one obtains

$$\Omega_0 t_r = (\pi + \rho) [1 + (\beta_1 \omega / \Omega_0) \delta], \quad (10a)$$

$$\Phi_r = -\Phi_s + (\beta_1 / \Omega_0^2) (\omega / \beta_2)^2 (\rho + \pi) \delta, \quad (10b)$$

with  $\rho = \arctan \beta_1 + \arcsin \beta_2$ ,  $\beta_1 = \omega / \Omega_0 \Phi_s$ , and  $\beta_2 = \omega / \sqrt{\omega^2 + \Phi_s^2 \Omega_0^2}$ . Having reached  $\Phi_r$ , the cutoff function in (4) forces the system to stay at rest until the maximum angle of repose  $\Phi_s$  is reached again. The duration time in the rest state is given by  $\Delta t = (1/\omega)(\Phi_s - \Phi_r)$ . The combination of the avalanche dynamics (the slip part) (9) and (10) and the motionless state (the stick part) determines one period of the slip-stick behavior of the system. This process will go on forever with a period  $T = t_r + \Delta t$ . (iv) Above  $\omega_T$ , the stick part of the dynamics no longer exists. For small  $\delta$  and  $\Omega_0$  of order unity,  $\omega_T$  is also small. Therefore, the relaxation time to the constant flow solution is very long (proportional to  $1/\delta\omega$ ), implying that just above  $\omega_T$  the dynamics consists of long-lived transient periodic oscillations in  $\Phi(t)$  and  $v(t)$ . They might be related to the ‘‘periodic’’ avalanches found in the experiment of Caponeri *et al.* [6]. (v) While slipping, the angle  $\Phi(t)$  can also reach values higher than  $\Phi_s$  and lower than  $-\Phi_r$ . This is caused by external rotation. In the lowest-order approximation, one finds that the maximum (minimum) angle  $\Phi_+$  ( $\Phi_-$ ) is given by  $\Phi_{\pm} = \pm \Phi_s [1 + (\omega / \Omega_0 \Phi_s)^2]^{1/2} + O(\delta)$ .

### VERTICAL VIBRATIONS

Our model also offers a simple, qualitative explanation for the logarithmic decay law of the angle  $\varphi$  in the presence of additional vertical vibrations [2]. Vertical vibrations dilate the granular system, particularly the surface layer. This can be incorporated in the model in an indirect way: The static limit of the dynamic friction coefficient in the presence of large variations becomes strongly diminished, i.e.,  $b_0 \rightarrow b_0^v \ll 1$  [13,14]. In addition, vibration drives the grains off the rest state even at

angles  $\Phi_{ss}$ , somewhat lower than  $\Phi_s$  [2]. This can be incorporated by a nonzero initial velocity of the grains,  $v(0) = \kappa$ , which is characteristic for a given experimental setup with fixed vibration amplitude and frequency. Let us now show that these general features can indeed lead to a topological change in the dynamics of (4). Benza, Nori, and Pla [9] have shown that the coupling coefficient  $a$  is proportional to  $\tan \varphi$  in finite cylinders. This implies that  $a = \hat{a} \tan \varphi_d$ , with  $\hat{a}$  being independent of  $\varphi_d$  in the lowest-order approximation. To understand the effect of vibration, it proves useful to scale (2) with  $\hat{a}$  instead of  $a$ . The structure of (4) is preserved and the coefficients are altered: With  $\varphi_d^v = \arctan(b_0^v)$  one obtains  $\delta \rightarrow \hat{\delta} = \delta / \tan \varphi_d^v = g b_2 \cos^2 \varphi_d^v / \hat{a} \sin \varphi_d^v$  and  $\Omega_0^2 \rightarrow \hat{\Omega}_0^2 = \Omega_0^2 \tan \varphi_d^v = \sin \varphi_d^v (1 + \tan^2 \varphi_d^v)$ . From that, one can see that  $\varphi_d^v \ll 1$  corresponds to  $\hat{\Omega}_0^2 \ll 1$  and  $\hat{\delta}$  large. In the limit  $\hat{\Omega}_0^2 \rightarrow 0$ , (3) reads  $\ddot{\Phi} - \hat{\delta}(\dot{\Phi} - \omega)^2 = 0$ , and can be solved analytically using initial conditions  $\Phi(0) = \Phi_{ss}$  and  $\dot{\Phi}(0) = -\kappa + \omega$ . The result reads

$$\Phi(t) = \Phi_{ss} + \omega t - (1/\hat{\delta}) \ln(1 + \hat{\delta} \kappa t). \quad (11)$$

The time evolution consists of two competing effects: a linear increase in time due to external rotation and a *logarithmic decay due to friction*. Let us discuss in particular the case  $\omega = 0$ . Then, one obtains precisely the logarithmic decay of  $\Phi$  as verified experimentally by Jaeger, Liu, and Nagel [2]. This fact is an indication of the validity of the friction law we propose because we find this characteristic logarithmic decay for other friction laws [6,8,9] only if we use a very small nonmonotonicity. In general,  $\Omega_0$  will not be exactly zero, but very close to zero. Then (11) is the leading-order solution in a perturbation expansion for small  $\Omega_0^2$ , which is valid on short- and intermediate-time scales. Higher-order terms in the perturbation expansion lead to corrections to the  $\ln(t)$  behavior. In the long-time limit,  $\Phi(t)$  will saturate at a value close to zero [13].

### CONCLUSIONS

Although the minimal model (4) is comparable simple, many basic features of the transition to flow in granular systems can be explained qualitatively. We emphasize the following. (i) A dynamic friction coefficient  $k_d(v)$ , which increases *monotonically* with  $v^2$ , is sufficient to understand surface flow of granular piles, particularly the periodic slip-stick flow, the almost periodic avalanches close to  $\omega_T$ , and the constant flow behavior found in the rotating-cylinder experiments of Caponeri *et al.* [6]. (ii) In the presence of vertical vibrations, the assumption that  $k_d(v \rightarrow 0)$  is strongly diminished can explain the fact that the angle of the pile decays, for not too long times, logarithmically in time [2]. Hence our deterministic approach is inherently able to describe the relaxation law of the surface angle of the pile without the need to invoke additional statistical concepts as done previously in Refs. [2,15]. We hope that our study will stimulate more experimental work aimed at investigating in greater detail the friction law that governs the dynamics in granular systems.

- [1] For a recent review see H. M. Jaeger and S. R. Nagel, *Science* **255**, 1523 (1992); S. R. Nagel, *Rev. Mod. Phys.* **64**, 321 (1992); P. Evesque, *Contemp. Phys.* **33**, 245 (1992), and references cited therein.
- [2] H. M. Jaeger, C. Liu, and S. R. Nagel, *Phys. Rev. Lett.* **62**, 40 (1989).
- [3] P. Evesque, *Phys. Rev. A* **43**, 2720 (1993), and references cited therein.
- [4] S. Douady, S. Fauve, and C. Laroche, *Europhys. Lett.* **8**, 621 (1989).
- [5] H. K. Pak and R. P. Behringer, *Phys. Rev. Lett.* **71**, 1832 (1993); G. W. Baxter, R. P. Behringer, T. Fagert, and G. A. Johnson, *ibid.* **62**, 2825 (1989).
- [6] M. Caponeri, S. Douady, S. Fauve, and C. Laroche, National Science Foundation Report No. NSF-ITP-92-140, 1992 (unpublished); S. Fauve, C. Larouche, and S. Douady, in *Physics of Granular Media*, 1991 Les Houches Lectures, edited by D. Bideau and J. Dodds (Nova Science, New York, 1991).
- [7] P. A. Thompson and G. S. Grest, *Phys. Rev. Lett.* **67**, 1751 (1991); T. Pöschel and V. Buchholtz, *ibid.* **71**, 3963 (1993); V. Buchholtz and T. Pöschel, *Physica A* **202**, 390 (1994), and references cited therein.
- [8] H. M. Jaeger, C. Liu, S. R. Nagel, and T. A. Witten, *Europhys. Lett.* **18**, 619 (1990). This model does not incorporate dynamical changes of the surface angle.
- [9] V. G. Benza, F. Nori, and O. Pla, *Phys. Rev. E* **48**, 4095 (1993).
- [10] R. A. Bagnold, *Proc. R. Soc. London, Ser. A* **225**, 49 (1954); **295**, 219 (1966).
- [11] Neglecting that  $\varphi$  is a dynamical quantity,  $\varphi_d$  is the angle where the acceleration  $\dot{v}$  of the particle would be zero, if in addition the dynamic friction coefficient would be constant (i.e.,  $b_2=0$ ).
- [12] See, e.g., P. B. Kahn, *Mathematical Methods for Scientists and Engineers* (Wiley, New York, 1990).
- [13] S. J. Linz and P. Hänggi, *Phys. Rev. E* **50**, 3469 (1994).
- [14] This can be understood using a simple model of an inelastic bouncing "ball" on a rough vibrating surface; for details see Ref. [13].
- [15] A. Metha, R. J. Needs, and S. Dattagupta, *J. Stat. Phys.* **68**, 1131 (1992).